

1 **Epigenetic heterogeneity after *de novo* assembly of native full-length Hepatitis**  
2 **B Virus genomes**

3  
4 Chloe Goldsmith<sup>1,2\*</sup>, Damien Cohen<sup>2</sup>, Anaëlle Dubois<sup>2</sup>, Maria-Guadalupe Martinez<sup>2</sup>, Kilian  
5 Petitjean<sup>3</sup>, Anne Corlu<sup>3</sup>, Barbara Testoni<sup>2</sup>, Hector Hernandez-Vargas<sup>4</sup>, Isabelle Chemin<sup>2\*</sup>

6  
7 1: INSERM U1052, CNRS UMR-5286, TGFB and immune evasion, Lyon Cancer Research  
8 Center (CRCL), Lyon, France

9 2: INSERM U1052, CNRS UMR-5286, Cancer Research Center of Lyon (CRCL), Lyon, France

10 3: Inserm, Univ-Rennes, INRAe, Institut Nutrition, Metabolism and Cancer (NuMeCan),  
11 UMR\_S 1241, Rennes, France

12 4: Centre Leon Berard (CLB), Lyon Cancer Research Center (CRCL), Lyon, France

13

14 \* Co-corresponding Authors

15 [Chloe.Goldsmith@lyon.unicancer.fr](mailto:Chloe.Goldsmith@lyon.unicancer.fr)

16 **Cancer Research Center of Lyon (CRCL), INSERM U1052**

17 **Centre Léon Bérard, 4th floor Cheney B,**

18 **28 Rue Laennec, 69373 Lyon Cedex 08, France**

19

20

21 **Key words:**

22 DNA methylation; Oxford Nanopore Technology; epigenetics; 5mC; HBV; 5mCpG; ONT;

23 HBV; cccDNA; cirrhosis; HCC

## 24 **Abstract**

25 Methylation of Hepatitis B Virus (HBV) DNA in a CpG context (5mCpG) can alter the  
26 expression patterns of viral genes related to infection and cellular transformation.  
27 Moreover, it may also provide clues to why certain infections are cleared, or persist with  
28 or without progression to cancer. The detection of 5mCpG often requires techniques that  
29 damage DNA or introduce bias through a myriad of limitations. Therefore, we developed a  
30 method for the detection of 5mCpG on the HBV genome that does not rely on bisulfite  
31 conversion or PCR. With cas9 guided RNPs to specifically target we enriched in HBV DNA  
32 from PHH infected with HBV Genotype A, E or D prior to sequencing with Nanopores  
33 MinION. In addition, we were also able to enrich and sequence HBV from patient liver  
34 tissue achieving coverage of ~2000x. Moreover, using the developed technique, we have  
35 provided the first *de novo* assembly of native HBV DNA, as well as the first landscape of  
36 5mCpG from native HBV sequences. Furthermore, the developed tools are scalable to the  
37 Nanopore Flongle device providing whole genome length HBV sequences in < 4h. This  
38 method is a novel approach that enables the enrichment of viral DNA in a mixture of  
39 nucleic acid material from different species and will serve as a valuable tool for infectious  
40 disease monitoring.

41

## 42 **Introduction**

43 HBV infection is divided into five clinical categories: asymptomatic, acute, chronic,  
44 fulminant, and occult. Occult HBV infection has been defined as the “presence of HBV  
45 viral DNA in the liver (with or without detectable HBV DNA in serum) of HBsAg-negative  
46 individuals tested with the currently available serum assays” (Raimondo et al. 2010,  
47 2019). Although the mechanism is not well understood, occult HBV infection is associated  
48 with liver pathogenesis, significantly increasing the risk for liver cirrhosis and  
49 hepatocellular carcinoma (HCC) (Ikeda et al. 2009; Mak et al. 2020; Perumal  
50 Vivekanandan et al. 2008). In addition, the overall degree of viral replication has been  
51 strongly linked to carcinogenesis (Chen 2006). Therefore, understanding factors that  
52 regulate HBV replication may provide insights into occult infection and preventing HCC.

53

54 HBV has a particular replication cycle that involves protein-primed reverse transcription  
55 of an RNA intermediate called pregenomic RNA (pgRNA) occurring in the nucleocapsid  
56 (Wang and Seeger 1993). Upon entry into hepatocytes, viral genomic DNA in the  
57 nucleocapsid is in the form of 3.2kb partially double stranded DNA, also called relaxed

58 circular DNA (rcDNA) (Summers, O'Connell, and Millman 1975). The rcDNA is then  
59 transported to the nucleus and converted into covalently closed circular DNA (cccDNA) by  
60 a still ill-defined mechanism. The HBV polymerase, responsible for reverse transcription,  
61 is encoded within the viral genome. The HBV polymerase lacks proofreading activity  
62 which results in a high amount of variability; several HBV genotypes have been  
63 characterized, named A to J, along with nearly 40 sub-genotypes that have varying  
64 characteristics and clinical implications. These different HBV genotypes can vary in their  
65 DNA sequence by up to 7.5% (Rajoriya et al. 2017). While our understanding of HBV DNA  
66 regulation is still limited, there some evidence that cccDNA could be epigenetically  
67 regulated (reviewed in (Xia and Guo 2020).

68

69 Recent studies have identified epigenetic modifications of HBV DNA, including methylated  
70 cytosines (5mC) as a novel mechanism for the control of viral gene expression (Pollicino  
71 et al. 2006). However, the current methods to detect modified bases have a number of  
72 limitations. Bisulfite modification has been considered the gold standard for the detection  
73 of 5mC for over a decade. This technique converts unmodified cytosines into uracil, and  
74 then the 5mC levels are deduced by difference (Li and Tollefsbol 2011). This technique  
75 leads to extensive DNA damage and introduces bias through incomplete conversion.  
76 Moreover, it is not able to distinguish the difference between 5mC and other modified  
77 bases that can occur in the same location (eg 5hmC). Thus, whilst this technique has  
78 been incredibly useful, there is a demand for the development of more direct measures of  
79 5mC. Moreover, current sequencing methods are not able to easily distinguish between  
80 different forms of HBV (rcDNA verses cccDNA) or identify episomal or integrated HBV  
81 DNA.

82

83 Nanopore sequencing is a unique, scalable technology that enables direct, real-time  
84 analysis of long DNA or RNA fragments (Madoui et al. 2015). It works by monitoring  
85 changes to an electrical current as nucleic acids are passed through a protein nanopore.  
86 The resulting signal is decoded to provide the specific DNA or RNA sequence. Moreover,  
87 this technology allows for the simultaneous detection of the nucleotide sequence as well  
88 as DNA and RNA base modifications on native templates (Jain et al. 2016); hence,  
89 removing introduced bias from sodium bisulfite treatment and PCR amplification.  
90 However, a first enrichment step of the target loci or species prior to sequencing is still  
91 necessary. Traditionally, this would be done by PCR amplification, however, this would of

92 course lead to a loss of modified bases like 5mC. Thus, development of enrichment  
93 techniques that do not degrade DNA or result in a loss of target bases is needed, in order  
94 to fully benefit from Nanopores ability to delineate 5mC levels on native DNA. Nanopore  
95 is also capable of sequencing long reads, and can potentially capture the whole HBV  
96 genome in single reads and thus provide the sequence information for single HBV  
97 molecules. Integration of the entire HBV genome has not been reported, therefore,  
98 sequencing HBV with Nanopore has the potential to distinguish between episomal and  
99 integrated HBV DNA. Furthermore, sequencing single HBV molecules could also identify  
100 the “gap” in rcDNA allowing discrimination between rcDNA and cccDNA forms of HBV.

101

102 In this work we developed a translatable method for the enrichment, sequencing, de novo  
103 assembly and the detection of modified bases in the HBV genome; determining the  
104 methylation landscape of different HBV genotypes *in vitro* as well as in patient liver  
105 tissue. We ascertained the HBV 5mCpG levels, for the first time, on directly sequenced  
106 native HBV DNA. These methods represent a valuable and highly novel tool for the  
107 detection of modified bases on viral genomes.

108

## 109 **Results**

### 110 **Enrichment**

111

112 Performing whole genome sequencing of HBV infected cells without any type of  
113 enrichment, achieves an extremely low sequencing depth with any sequencing platform.  
114 We performed whole genome sequencing of HBV infected PHH with Nanopore’s MinION  
115 and only 1x of HBV was obtained (data not shown). This is due to the size of HBV genome  
116 compared to the contaminating host (3.2KB verses 3.2GB, HBV=0.000001% of available),  
117 thus enrichment of HBV is clearly necessary. We utilized Cas9 guided Ribonucleic proteins  
118 (RNPs) to linearize and enrich in HBV DNA from the total DNA extracted from HBV infected  
119 Primary Human Hepatocytes (PHH). This method has been described previously to enrich  
120 in target loci in the human genome (Gilpatrick et al. 2020), and to our knowledge, the  
121 present study is the first evidence that this approach can be used to sequence viral or  
122 circular DNA (figure 1A). This method allows HBV genome enrichment without PCR  
123 amplification, thus allowing sequencing of native DNA taking full advantage of the ability  
124 of Nanopores to detect modified bases. Briefly, starting material consisted of positive and  
125 negative controls for HBV methylation, total DNA extracted from PHH infected with

126 different genotypes (GA, GD or GE) or DNA from fine needle liver biopsies of HBV infected  
127 patients (figure 1A). Available DNA ends were blocked by dephosphorylation with calf  
128 intestinal phosphatase, this step is essential to prevent the nuclear DNA from being  
129 available for the ligation of adapters in later steps. We then used 2 sgRNAs in a highly  
130 conserved region, to target the HBV genome, one for the positive strand and an  
131 additional guide for the negative strand (figure 1A). Use of 2 gRNAs leading the positive  
132 and negative strand was critical, since the RNP complex remains attached to the strand  
133 where it makes the cut, making the other strand available for the ligation of adapters  
134 allowing the sequencing of both the positive and negative strands. After the adapters and  
135 motor proteins were ligated to the newly available DNA ends, the libraries were loaded  
136 onto the MinION device and DNA sequencing occurred in a 5' to 3' directionality on a  
137 MinION R9.4.1 flow cell.

139

140

#### 141 **Yield and coverage**

142 In order to determine the necessary sequencing depth to detect differential HBV DNA  
143 methylation, we combined reads from the positive and negative controls for methylation  
144 to obtain specific coverage (10x, 40x, 100x and 1000x) and percentages of methylation  
145 (0, 25, 50, 75, 100%) We then determined methylation using Nanopolish and the  
146 minimum coverage was defined when a significant difference was detectable in each  
147 group of percentage methylation (figure 1B) (Full list of p-values in supplementary table  
148 1). Interestingly, even at the lowest level of coverage (10x) we observed a clear  
149 difference between the 0% and 75% and 100% methylation levels ( $p < 0.05$ ), however,  
150 distinguishing between 25% and 50% was not possible at this level of coverage. At a  
151 coverage of 40x, a significant difference in 5mCpG levels between each percentage  
152 methylation group was observed, and as such, 40x was identified as the minimum  
153 sequencing depth required for detection of HBV methylation.

154

155 Starting with DNA extracted from HBV infected PHH or infected patient tissue, we utilized  
156 our cas9 enrichment protocol to linearise and sequence the HBV genome. The total yield  
157 ranged between 150-200K reads collecting in the range of 1-2 GB of DNA, our aligned  
158 read length was ~2.5KB (N50 = ~2520, median read length = ~2310) (supplementary  
159 figure 1A). Raw reads were basecalled with Guppy (Version 4), a draft assembly was  
160 generated with Canu and polished with Medaka. The resulting consensus sequence was

161 used to align the basecalled reads and calculate HBV genome coverage (figure 1C and  
162 1D) and enrichment. We obtained a clear enrichment of HBV with up to 3000x coverage  
163 for certain HBV genotypes which, was comparable with total HBV detected in the same  
164 samples by qPCR and variability in the sequencing depth can explained by infection  
165 efficacy. Calculated with pycoQC (Leger and Leonardi 2019), ~5% of all reads were on  
166 target (supplementary figure 1), which is a clear enrichment for this particular technique  
167 considering the very low levels of HBV detected with whole genome sequencing.  
168 Significantly, the gap present in the positive strand of rcDNA was identified in this  
169 analysis (supplementary figure 1). Levels of infection of the PHH used in this experiment  
170 were evaluated by qPCR, which established a high level of infection (figure 1C, 1D and  
171 supplementary figure 1). Given the high copy numbers of viral DNA, and thus replicative  
172 intermediates, it was expected to find this range in the length of the gap present in the  
173 positive strand of rcDNA, with a clear tapering of read length; this could be at least  
174 partially due to the different stages in the transcription of HBV DNA (supplementary figure  
175 1). However, the lower coverage for the negative strand is likely due to the difference in  
176 efficacy of the sgRNA guides. Despite the differences in frequency, we were clearly able  
177 to sequence both strands of native HBV with cas9 enrichment technique at a coverage  
178 considered highly satisfactory for the identification of HBV methylation.

179

## 180 **Nanopore Flongles capable of sequencing native HBV in a mixture of viral and** 181 **host DNA**

182 In order to develop a more affordable and translatable method for the identification of  
183 HBV DNA in a mixture of viral and host DNA, we ambitioned to test our method on the  
184 smaller and cheaper Nanopore flow cells “Flongles”. Using these smaller flow cells  
185 allowed us to start with less DNA (0.5-1ug). This is an important consideration for clinical  
186 translation of this method since obtaining large quantities of DNA from tissue/ liquid  
187 biopsies is not be feasible. After 4h of sequencing we generated 367 reads totaling 1.3MB  
188 of sequencing data. 100 reads passed QC, 10% of which aligned to the HBV genome.  
189 However, we must note that the reads obtained from the flongle were of a much lower  
190 quality than those sequenced with the MinION flow cells (supplementary figure 2). While  
191 this was likely due to the lower molarity of DNA available for sequencing causing an  
192 increase in the speed at which DNA passes through the nanopores, causing a drop in  
193 translocation speed, it is, nonetheless, an important consideration for the potential  
194 applications of this technique. As expected, by using Flongles and starting with a lower

195 quantity of starting material, we obtained lower coverage (~10x) of the HBV genome  
196 than by using the larger and more expensive MinION flow cells (figure 1C). While our  
197 analysis to detect methylation differences indicated that 40x is the minimum required  
198 coverage to detect between 25% and 50% methylation, at a coverage of 10x we were  
199 able to significantly identify differences between 0% and 25% methylation, as well as  
200 75% and 100% methylation. Thus a coverage of 10x for certain applications could be  
201 considered sufficient as is also the case for other techniques using short read sequencing  
202 (Olkhov-Mitsel and Bapat 2012) and long read sequencing (Gigante et al. 2019).  
203 Importantly, the same amount of starting material would have resulted in far greater  
204 coverage on the larger minION flow cell; however, while Nanopore is less expensive than  
205 other high throughput sequencing, the even lower price point of Flongle flow cells is an  
206 attractive alternative. Thus, our data suggests that our method can be applied to enrich  
207 HBV DNA in samples for sequencing with Nanopores 'Flongles' to obtain rapid detection  
208 of HBV in laboratory infection models.

209

### 210 **Nanopore sequencing detects HBV 5mCpG**

211 We next sought to determine the validity of using Nanopores to detect modified bases in  
212 the HBV genome. Beta values for each CpG site were calculated by Nanopolish (Simpson  
213 et al. 2017) and plotted with methplotlib (De Coster, Stovner, and Strazisar 2020) (figure  
214 2). Because nanopore sequencing directly evaluates methylation patterns on native DNA  
215 strands, we are able to observe long-range methylation information on each DNA  
216 molecule. As anticipated, very low levels of methylation were observed in the negative  
217 control with some residual methylation and background noise detected (figure 2A).  
218 Interestingly, we identified some single reads that were methylated in the negative  
219 control, likely a result of the presence of residual un-amplified DNA; thus, we determined  
220 that low levels of methylation observed were partially attributed to this contaminating  
221 starting material. However, we also identified random methylated CpG sites throughout  
222 reads in the fully unmethylated control. These could also be due to methylation calling  
223 errors and can therefore be considered as background noise for the technique. In the  
224 positive control we detected high levels of DNA methylation (figure 2A). However, there  
225 was variability in the average levels of 5mCpG. After visualising the methylation of the  
226 single molecules, we identified a number of reads that were not fully methylated which  
227 was likely contributing to the lower average levels of 5mCpG at certain loci. These  
228 unmethylated reads are likely attributed to the efficiency of the Methyltransferase in the

229 preparation step of the fully methylated control. However, in a similar way to the  
230 unmethylated control, there was also some random CpG sites throughout the data that  
231 were not methylated in the positive control, which is more likely attributed to methylation  
232 calling errors. In order to address the issue of introduced bias through methylation callers,  
233 in addition to calling 5mCpG with Nanopolish, we validated our findings with an additional  
234 methylation caller, Guppy. Spearman's correlation of the methylation levels obtained for  
235 the fully methylated and unmethylated HBV controls with Nanopolish and Guppy +  
236 Medaka, indicated a highly significant correlation ( $R = 0.83$ ,  $p < 2.2e^{-16}$ ) (figure 2E).

237  
238 In order to validate our findings obtained with Nanopore, we developed a bisulfite  
239 quantitative methyl-specific qPCR assay (BS-qMSP). Briefly, DNA from controls and  
240 genotype D samples were bisulfite converted, followed by methyl-specific qPCR, with  
241 methyl specific primers designed for 6 CpG sites in the HBV genome. Beta Values were  
242 calculated by comparing the % of methylated DNA to the total (unmethylated +  
243 methylated DNA). (Figure 2B). As expected, beta values were comparable for all CpG sites  
244 in the methylated, unmethylated controls and samples, and exhibited a high correlation  
245 coefficient (0.96,  $P < 0.05$ ) (figure 2D).

246  
247 The clear extremes observed in the different controls (figure 2A) ( $> \sim 90\%$  methylation in  
248 FM,  $< \sim 10\%$  methylation in the FU) validated in multiple methylation callers (figure 2E),  
249 and with an additional technique (figure 2B, 2D), indicate the efficacy of Nanopore  
250 technology for the detection of 5mCpG on HBV DNA. We were therefore highly confident  
251 in this tool for the detection of 5mCpG levels on the HBV genome.

### 252 253 **Absence of DNA methylation observed in HBV virions**

254 After identifying the background noise levels of 5mCpG identified in synthetically fully  
255 methylated and unmethylated HBV DNA, we next sought to determine the 5mCpG levels  
256 in an expected biologically negative control, HBV Virions. HBV DNA is reverse transcribed  
257 after being packaged in the viral capsid in the cytosol of the infected cells, thus out of  
258 touch with DNA methyltransferase enzymes and as a result, likely not methylated (Wang  
259 and Seeger 1993). Overall, there were very low levels of 5mCpG identified in the HBV  
260 virions, comparable to the amplified HBV control (figure 2A). These levels were not higher  
261 than those detected in the unmethylated HBV control (figure 2C), and as such, were likely  
262 a result of methylation calling errors or potentially some contaminating DNA from dead

263 cells also collected during the HBV viral particle purification process. Regardless, the  
264 levels were still very low (<15%). Taken together with the methylation levels in the  
265 amplified, unmethylated HBV control, these levels of 5mCpG indicate the background  
266 noise levels of the detection method. Moreover, these data continued to increase our  
267 confidence in Nanopore sequencing to accurately detect 5mCpG in the HBV genome.

268

### 269 **Basal levels of HBV 5mCpG in infected PHH with different genotypes**

270 In order to determine the basal levels of 5mCpG in HBV infection models *in vitro*, we used  
271 primary human hepatocytes (PHH) infection model, which is the gold standard HBV in  
272 vitro infection model. PHH were infected with a viral inoculum of HBV genotypes A, D and  
273 E and collected nuclear DNA from cells 6 days post infection. Infection efficiency was  
274 determined by HBsAg and HBeAg expression by ELISA as well as total HBV DNA in the  
275 supernatant by qPCR every 3 days. We observed similar infection rates for HBV Genotype  
276 D and E, however, for genotype A all parameters were negligible, indicating lower  
277 infection rates (supplementary figure 1). Despite the negligible levels detected for the  
278 infection efficacy of HBV genotype A, our cas9 enrichment technique was able to enrich  
279 and sequence HBV genotype A with ~80x coverage (figure 1C). In addition, our cas9  
280 technique was highly effective at enriching HBV of all genotypes tested at sufficient  
281 coverage to evaluate methylation levels.

282

283 Detected 5mCpG levels were comparable across the different HBV genotypes (figure 2F-  
284 H). We observed low levels of 5mCpG across the three genotypes tested with HBV  
285 genotype E having the highest basal levels across the genome (figure 2C). While we did  
286 not identify any differentially methylated loci when comparing the different genotypes,  
287 the technique developed was clearly able to enrich and sequence all genotypes tested.  
288 Moreover, the distribution of methylation for each of the different genotypes was  
289 significantly different from both of the negative controls (figure 2C) and from each other.  
290 Interestingly we also identified an enrichment of 5mC in the preS1/ preS2 region for each  
291 of the genotypes and could thus have implications for HBS expression. These differences  
292 in 5mC distribution taken together with the different pattern of methylation frequency  
293 (figure 2F-H) indicate that HBV genotypes exhibit genotype specific 5mC landscapes.  
294 Thus, these data further add to the efficacy of the cas9 sequencing technique for the  
295 enrichment and delineation of HBV methylation in a laboratory setting.

296

## 297 **Enrichment and sequencing of HBV in infected patients identifies epigenetic** 298 **heterogeneity**

299

300 In order to test the efficacy of our technique and its potential for translational research in  
301 clinics, we proceed to test cas9 enrichment and sequencing in HBV DNA from patient  
302 tissue. We took advantage of samples collected as part of the PROLIFICA study (Lemoine  
303 et al. 2016). We used 900ng of DNA obtained from a HBV positive patient's liver biopsy.  
304 All viral parameters were assessed including pgRNA and quantification of cccDNA  
305 (supplementary Table 2). By using our cas9 sequencing technique we were able to enrich  
306 in enough HBV specific reads to perform a *de novo* assembly. The HBV genotype was  
307 determined by jumping profile Hidden Markov Model (jpHMM) and identified as genotype  
308 A, and after alignment, identified over 2000x coverage of this HBV genome (figure 1C and  
309 1D). The methylation of CpG sites was determined and the average 5mCpG levels were  
310 calculated (figure 2I). Interestingly, certain CpG sites were around 50% methylated across  
311 the HBV genome. Visualization of the single HBV DNA molecules revealed heterogeneity  
312 in the methylation levels, indicating the potential existence of differentially methylated  
313 HBV populations within the patient (figure 3). In order to explore this data further, we  
314 evaluated the distribution of HBV methylation levels in the patient sample. We observed a  
315 significant difference in the distribution of 5mCpG compared to both the fully methylated  
316 and fully unmethylated controls (figure 2C). Visualization of the 5mCpG distribution of  
317 individual reads (figure 3A) revealed heterogeneity of HBV molecules. Unsupervised  
318 hierarchical clustering of whole HBV molecules, identified 4 distinct clusters (figure 3B-C),  
319 suggesting that within the 1 patient, up to 4 epigenetically distinct HBV phenotypes exist.  
320 Whilst the differences between clusters was not identified as a particular region, there  
321 were certainly several CpGs that displayed large differences between groups. In particular  
322 CpG in the preS1/ preS2 S region that displayed the large differences between clusters  
323 (figure 3D and 3E). While, these data need to be confirmed with additional patients to  
324 conclude more broadly, it is not entirely surprising; HBV replication intermediates and  
325 virions were not methylated, and the methylation levels observed are likely due to the  
326 presence of cccDNA. An understanding of the epigenetic landscape of different HBV DNA  
327 populations is important when considering HBV regulation and occult infection. Taken  
328 together, these data highlight the potential of this technique in the enrichment and  
329 sequencing of HBV as well as analysis of HBV DNA methylation in clinical settings.

330

331

332

333

## 334 **Discussion**

335 Mapping the methylation of HBV DNA in infected cells can alter the expression patterns of  
336 viral genes related to infection and cellular transformation (Fernandez et al. 2009; Guo et  
337 al. 2009) and may also aid in understanding why certain infections are cleared, or persist  
338 with or without progression to cancer (Mirabello et al. 2012). Furthermore, the clear  
339 detection of viral methylation patterns could potentially serve as biomarkers for diseases  
340 that are currently lacking, including occult HBV infection (Nakamura et al. 2020).  
341 However, development of more sensitive high throughput techniques translatable to the  
342 clinic, is essential. The present study developed a technique to enrich and sequence HBV  
343 without the need for bisulfite conversion or PCR using cas9 guided RNPs coupled with  
344 Nanopore sequencing. We were able to enrich and sequence HBV from both infected PHH  
345 and patient liver tissue achieving coverage of ~2000x providing the first *de novo*  
346 assembly of native HBV DNA, as well as the first landscape of 5mCpG from native HBV  
347 sequences. By using nanopore we also took advantage of sequencing entire HBV  
348 genomes and identified several HBV epigenotypes in patient tissue.

349

350 The cas9 enrichment technique was first designed to enrich in target regions in the  
351 human genome prior to sequencing (Gilpatrick et al. 2020). We have adapted this method  
352 to enrich in viral DNA in a mixture of host DNA. The coverage obtained for the previous  
353 study was ~400x by using a triple cutting approach, whereby six or more sgRNAs were  
354 designed for each region of interest. By using just 2 sgRNAs targeting the HBV genome,  
355 we obtained much higher coverage than in the previous study and dramatically reduced  
356 the cost/ sample. We have attributed this to the smaller size of the HBV genome  
357 compared to the average sized regions the authors were targeting (3.2kb v 20kb) as well  
358 as the higher concentration of HBV genomes/ cell. Thus, it is not entirely surprising that  
359 the coverage was improved by such a large factor (>25x).

360

361 The developed technique enriches for episomal HBV DNA and can also somewhat  
362 distinguish between the different HBV forms. We first blocked linear DNA ends by  
363 phosphorylation and then linearized HBV with cas9 guided RNPs, after sequencing we  
364 selected reads that were less than 4000bp to perform a *de novo* assembly. In doing so,

365 we were sure to remove any integrated HBV reads that were sequenced, increasing  
366 specificity for episomal HBV. Moreover, we identified the “gap” in the positive strand of  
367 HBV. Therefore, during post-sequencing analysis, by selecting only HBV reads that cover  
368 the whole genome we identified those reads that correspond to cccDNA’s positive strand.  
369 However, since there is no gap in the negative strand of HBV rcDNA we can not  
370 distinguish it from cccDNA in this way. Other techniques to study rcDNA and cccDNA are  
371 limited. Southern Blot remains the gold standard for quantification of cccDNA, however it  
372 is time consuming and not practical for a large number of samples (Xia et al. 2017). Other  
373 techniques rely on PCR but show limited specificity when excess replication intermediates  
374 are present. Furthermore, HBV is renowned for its genomic sequence variability, with  
375 different genotypes varying as much as 7.5% (Rajoriya et al. 2017) which can prove  
376 difficult for the design of primers. Our cas9 enrichment protocol was capable of  
377 sequencing all HBV genotypes tested. This is likely due to the conservation of the region  
378 used for the guides designed to specifically target HBV DNA which was not bound by  
379 polymerase kinetics. Our cas9 technique was also capable of enriching in HBV from  
380 patient liver tissue achieving over 2000x coverage of the HBV genome and thus  
381 demonstrating the potential of this technique in translation to clinical applications.

382

383 Current strategies for DNA methylation determination include bisulfite conversion  
384 followed by Sanger sequencing or methyl specific PCR, enzyme digestion assays and  
385 single-molecule, real-time (SMRT) sequencing (Olkhov-Mitsel and Bapat 2012). It is  
386 difficult to compare the efficiency of different techniques for detecting DNA methylation,  
387 since they are all valuable for different applications; despite this, thorough reviews and  
388 comparisons have been conducted previously with limitations for each platform well  
389 described (Olkhov-Mitsel and Bapat 2012). Our technique was capable of detecting  
390 5mCpG in native HBV DNA from different genotypes *in vitro*, as well as in patient liver  
391 tissue. An advantage of our cas9 enrichment technique compared to traditional bisulfite-  
392 based sequencing methods is the clear benefit of sequencing native DNA that does not  
393 require Bisulfite conversion. Bisulfite conversion results in DNA degradation and,  
394 importantly, is not capable of distinguishing 5mC from other modified bases such as  
395 5hmC, whereas Nanopore based techniques are able to do so. In addition, with this  
396 nanopore technique we are able to simultaneously elucidate the DNA sequence and the  
397 single molecule methylation, while other techniques like Bisulfite conversion followed by  
398 methyl specific PCR require additional experimental analysis to ascertain the sequence

399 information. Furthermore, by sequencing full HBV reads we are able to identify the  
400 heterogeneity of HBV sequences making it possible to identify certain reads that are  
401 displaying differential methylation patterns within the sample population, another  
402 application that is not possible with existing techniques. The exception of course is SMRT  
403 sequencing. However, this technique has prohibitively expensive set up and ongoing  
404 costs compared to Nanopore, making it unfeasible for rapid deployment and set up of  
405 viral monitoring potentially in remote locations. In comparison, Nanopore is light, easy to  
406 handle and by using Flongles we obtained whole genome length HBV sequences in < 4h.

407

408 While the nanopore platform has clear benefits there are also several limitations.  
409 Importantly, a large quantity of starting material is required for this technique (1-5 $\mu$ g of  
410 DNA). While this is true on paper, we were able to achieve 2000x coverage of HBV with  
411 900ng of starting material (liver tissue from a HBV infected patient). On average our  
412 Patient liver tissue biopsies are less than 25mg and depending on the DNA extraction  
413 technique we can obtain up to 1-2 $\mu$ g of DNA. However, for other patient samples such as  
414 blood and plasma it is simply not possible to obtain large quantities of DNA. As such, PCR  
415 and bisulfite-based methods must be preferred. Nevertheless, with the development of  
416 the smaller nanopore Flongles and the continually improving bioinformatics and machine  
417 learning applications (Payne et al. 2020) it will soon be feasible to combine our technique  
418 with bioinformatic approaches to enrich in viral DNA from much lower quantities of  
419 starting material.

420

421 While we have focused on the application of this technique for detecting modified viral  
422 DNA bases, this tool can also be useful for other approaches; including the identification  
423 of mutations and tracking viral evolution, investigate transmission chains, the likes of  
424 which were observed in the Ebola outbreak in West Africa (Quick et al. 2016) and more  
425 recently in the COVID-19 pandemic of 2020 (Viehweger et al. 2019). By sequencing  
426 native reads and performing a *de novo* assembly, introduced bias from PCR amplification  
427 is eliminated. However, nanopore sequencing is still considered error prone with the raw  
428 read accuracy varying depending on several factors such as flow cell type, starting  
429 material quality, basecaller, basecalling speed, polishing etc. In optimal conditions,  
430 nanopore sequencing has a reported raw read accuracy of ~97% using flow cells with the  
431 R9.4 pore chemistry, while, the consensus accuracy and single molecule consensus  
432 accuracy is usually around 99.98% (Q37) (Lu, Giordano, and Ning 2016). In the present

433 study, our *de novo* assembly of native HBV reads generated a consensus with per-base  
434 99.9% similarity to existing HBV genotype D references generated with illumina  
435 sequencing (supplementary figure 1C), which is comparable to the benchmark values for  
436 the assembler used (Canu) (Koren et al. 2017; Nurk et al. 2020). Accurate references are  
437 imperative to improve the accuracy of downstream analysis, such as methylation calling.

438

439 Furthermore, there is huge potential for nanopore technology and the identification of  
440 additional modified bases. Since only low levels were observed and only 1 patient biopsy  
441 was screened in the present study, we were not able to correlate methylation with  
442 functional outcomes such as expression of viral parameters. That being said, the study of  
443 epigenetics is still in its infancy. Recently we found that levels of 5hmC in gene bodies in  
444 differentiating hepatocytes is highly correlated with the expression of those genes  
445 (Rodríguez-Aguilera et al. 2019). Thus, there is still a lot more to discover regarding the  
446 function of modified bases. However, the first point of call is accurate detection, and  
447 more work is needed to develop machine learning tools to detect, and benchmark  
448 additional modified bases in native Nanopore data.

449

## 450 **Conclusions**

451 We developed a sensitive and high throughput method for the enrichment and nanopore  
452 sequencing of native HBV DNA from infected PHH and patient liver tissue. This method is  
453 a novel approach that achieved a clear enrichment of viral DNA in a mixture of virus and  
454 host DNA without the need for PCR amplification. By sequencing native HBV DNA with  
455 nanopore we were also able determine the DNA methylation landscape of HBV without  
456 the use of bisulfite conversion. Moreover, using the developed technique, we have  
457 provided the first *de novo* assembly of native HBV DNA, as well as the first landscape of  
458 5mCpG from Naive HBV DNA. More work is needed to test compatible machine learning  
459 enrichment techniques to further improve the minimum required concentration of  
460 starting material.

461

## 462 **Methods**

### 463 *Cultivation of PHH*

464 Primary Human Hepatocytes (PHH) were extracted and maintained as previously  
465 described (Ancey et al. 2015).

466

467 *HBV cultivation and infections*

468 HBV inocula was generated as previously described (Ancey et al. 2015; Lucifora et al.  
469 2011). PHH were naturally infected with HBV genotype A, D and E for 24h (MOI 100). A  
470 stable infection was achieved after 3 days, cells were maintained for up to 14 days.  
471 Infection efficacy was determined by quantification of Hepatitis B surface antigen (HBsAg)  
472 and Hepatitis B e antigen (HBeAg) concentration in supernatant by ELISA and calculation  
473 of HBV copies/ $\mu$ L by qPCR as previously described (Ancey et al. 2015).

474

475

476 *Patient liver tissue*

477 Patient samples were collected as a part of the PROLIFICA study (Cohen et al. 2020;  
478 Lemoine et al. 2016). DNA was extracted from snap frozen human liver needle biopsies.  
479 Liver samples were first homogenized on ice using a TissueRuptor (Qiagen, Hilden,  
480 Germany) in homogenization buffer (Tris HCl pH 8, 50 mM; EDTA 1 mM; NaCl 150 mM)  
481 and then processed for DNA extraction.

482

483 *DNA extraction*

484 Cells, or homogenized tissues were digested with proteinase K prior to DNA isolation  
485 using MasterPure™ DNA Purification Kit (Epicentre, by Illumina, Madison, United States)  
486 according to manufacturer's instructions.

487

488 *Quantification of total HBV-DNA, cccDNA and pregenomic(pg) RNA in liver sample*

489 Quantification was performed using the QX200™ Droplet Digital PCR System (BioRad,  
490 Hercules, California, USA) with primers and fluorescence dual hybridization probes  
491 specific for total HBV-DNA or cccDNA as described in (Lebossé et al. 2017; Testoni et al.  
492 2019). Before cccDNA amplification, DNA was treated with 10U of Plasmid-safe Dnase  
493 (Epicentre® Illumina) for 45 minutes at 37°C following the latest update of the  
494 international working group on cccDNA standardization (Allweisset al., 2017 International  
495 HBV Meet-ing, O-45). Serial dilutions of a plasmid containing an HBV monomer (pHBV-  
496 EcoR1) served as quantification standard. To normalize the number of viral copies per cell  
497 content, the number of cellular genomes was determined using the b-globin genekit  
498 (Roche Diagnostics, Mannheim, Germany). Patient sample was independently analyzed in  
499 duplicate. The range of quantification was comprised between  $10^1$  and  $10^7$  copies of HBV  
500 genome/well for both cccDNA and total HBV-DNA assays. For pgRNA detection, specific

501 primers and Taqman® hybridization probe were used, as described in (Lebossé et al.  
502 2017; Testoni et al. 2019). The patient sample was independently analyzed in duplicate  
503 and pgRNA relative amount was normalized over the expression of housekeeping the  
504 gene GUSB (Hs99999908\_m1, Thermo Fisher Scientific, Waltham, MA, USA).

505

#### 506 *Laboratory assays*

507 HBsAg was detected by chemiluminescent microparticle immunoassay (Architect, Abbott)  
508 in 2012–2013 (Njai et al. 2015). HBV DNA levels were measured at the end of the Prolifica  
509 study in stored serum samples using in-house quantitative real-time PCR (detection limit:  
510 50 IU/mL), calibrated against an international standard (Ghosh, Sengupta, and Scaria  
511 2014).

512

#### 513 *Fully unmethylated and fully methylated controls*

514 HBV DNA was amplified by nested PCR as previously described to prepare a negative  
515 (fully unmethylated) control. After amplification, a positive control for methylation (fully  
516 methylated) was prepared by methylating CpG dinucleotides; by incubating 1µg of DNA  
517 with S-Adenosyl methionine (SAM) (32µM) with CpG Methyltransferase (M.SssI) (4-25  
518 units) (New England BioLabs) at 37°C for 1h before heating to 65°C for 20mins.

519

#### 520 *Nanopore library prep and sequencing*

521 DNA (0.5–3µg) from each sample or control was enriched in HBV and linearized using cas9  
522 guides RNPs. TracrRNA and crRNA (5'AGCTTGGAGGCTTGAACAGT3' and  
523 5'TAAAGAATTTGGAGCTACTGTG3') were purchased from Integrated DNA Technologies  
524 (IDT). Samples were barcoded and multiplexed using the Nanopore Ligation Sequencing  
525 kit (SQK-LSK109) and Native barcode expansion kit according to manufacturer's  
526 instructions (Oxford Nanopore Technology, Oxford UK). Sequencing was conducted with a  
527 Minion sequencer on ONT 1D flow cells (FLO-min106) with protein pore R9.4 1D chemistry  
528 for 24h or on a Flongle (FLO-106) for 4h Oxford Nanopore Technology, Oxford UK). Reads  
529 were basecalled with Guppy (version 4).

530

#### 531 *De novo assembly*

532 Basecalled fasQ files were used to assemble the HBV genome with canu (Koren et al.  
533 2017), that was polished using Medaka; a tool to create a consensus sequence from  
534 nanopore sequencing data using neural networks applied from a pileup of individual

535 sequencing reads against a draft assembly. Basecalled FastQs were then aligned to the  
536 generated consensus sequence using Minimap2 (Li 2018). Assembly was assessed by  
537 using BLAST (Zhang et al. 2000) which returned a 99.9% similarity score to existing HBV  
538 genotype D references and jumping profile Hidden Markov Model (jpHMM) which correctly  
539 identified the genotypes (supplementary figure 1C).

540

#### 541 *Methylation calling*

542 We first determined the methylation status of each CpG site on every read by using the  
543 widely used tool, nanopolish (Simpson et al. 2017) used recently by (Gigante et al. 2019).  
544 For validation, we also called DNA methylation using novel tool, Guppy (version 4). CpG  
545 Islands were predicted using MethPrimer .

546

#### 547 *Bisulfite (BS) and quantitative methyl specific PCR (qMSP)*

548 BS and qMSP protocols made available as detailed methods at protocols.io (Hernandez  
549 and Goldsmith n.d.). Primer sequences are available in supplementary table 3. Primers  
550 were designed with MethPrimer and purchased from Thermo Fisher Scientific (Waltham,  
551 MA, USA).

552

#### 553 *Statistics*

554 Data processing and statistic analyses were performed in R bioconductor. Differential  
555 methylation was determined by Dispersion shrinkage for sequencing data (DSS) as  
556 previously described (Gigante et al. 2019; Park and Wu 2016). Kruskal-Wallis one-way  
557 analysis of variance was used to determine differences in average methylation levels.  
558 Significance value =  $p < 0.01$ . Hierarchical clustering was performed by k-means cluster  
559 analysis using d-Ward Hierarchical clustering with the euclidean method, number of  
560 groups determined by the elbow method.

561

#### 562 *Converting reads for visualization in IGV*

563 In order to take advantage of the single molecule sequencing with Nanopore, we  
564 converted the reads for visualization using Methplotlib (De Coster et al. 2020).

565

#### 566 *Data availability*

567 All raw and processed sequencing data is has been made publicly available with GEO  
568 (Ascension numbers: GSE162518, GSM4953612, GSM4953613, GSM4953614,

569 GSM4953615, GSM4953616, GSM4953617). Assembled HBV sequences made available in  
570 GeneBank Submission ID # 2386637.

571

572

573 *Conflict of interest*

574 Chloe Goldsmith and Hector Hernandez have received travel and accommodation support  
575 to attend conferences for Oxford Nanopore Technology.

576

577 *Acknowledgements*

578 The Authors would like to thank the patients that participated in this study and also  
579 acknowledge the whole Inserm U1052 team for any help along the way.

580

581 *Funding*

582 This work was supported by the Agence Nationale de Recherches sur le SIDA et les  
583 Hépatites Virales (ANRS, Reference No. ECTZ47287 and ECTZ50137); La Ligue  
584 Nationale Contre Le Cancer Comité d’Auvergne-Rhône-Alpes AAP 2018.

585

586 *Ethics approval and consent to participate*

587 Pre-test counseling was delivered and written consent obtained. Ethics approval for the  
588 study was granted by the Government of The Gambia and MRC Gambia Joint Ethics  
589 Committee.

590

591 *Authors’ contributions*

592 CG generated concepts, completed experiments, performed analysis and wrote the  
593 manuscript: DC and AD completed experiments: GM assisted in concept generation  
594 and manuscript preparation: BT assisted in manuscript preparation: KP assisted in  
595 manuscript preparation: AC obtained funding and assisted in manuscript preparation:  
596 HH performed analysis and obtained funding: IC assisted in manuscript preparation  
597 and obtained funding. All authors have discussed the results and read and approved  
598 the manuscript.

599

## 600 **Figure legends**

601

602 **Figure 1.** Optimal coverage of HBV for detection of HBV methylation with Nanopore.

603 **A:** Overview of sampling and cas9 targeted sequencing protocol adapted for circular  
604 viral genomes. Briefly, all available DNA ends were dephosphorylated prior to  
605 liberation of target sites by cutting with cas9 guided RNPs. The circular viral genome  
606 was then linearized and prepared for the ligation of adapters and motor proteins.  
607 Libraries were then loaded onto a MinION to be sequenced with Nanopores. **B:**  
608 calculation of optimal coverage for HBV methylation detection. Briefly, reads from  
609 sequencing positive and negative controls for HBV methylation were pooled to  
610 achieve 10-1000x coverage and 0, 25, 50, 75 or 100% methylation. Methylation was  
611 called with Nanopolish. **C:** Sequencing depth achieved with nanopore (reads aligning  
612 to genome) compared to total HBV detected by qPCR (copies of HBV detected by  
613 qPCR). **D:** Coverage of HBV genome from patient tissue (P1) after enrichment via  
614 cas9 sequencing technique with MinION flow cell, x-axis is HBV genome length  
615 (3.2KB).

616

617 **Figure 2.** HBV methylation levels in HBV. **A:** Average methylation of HBV Controls  
618 and single molecule visualization of first 100 reads using methplotlib, **B:** 5mC levels  
619 of 6 CpG sites detected by 2 techniques; Nanopore sequencing and qMSP. **C:**  
620 Distribution of 5mC in HBV from PHH infected with different genotypes (GA, GD and  
621 GE) and isolated from patient tissue (P1). **D:** Correlation of 5mC levels obtained with  
622 qMSP with Nanopore, samples + controls. **E:** Correlation of 5mC levels detected with  
623 different methylation callers, Nanopolish and Guppy. **F-I:** Methylated frequency and  
624 single molecule visualization of HBV from infected PHH (**F**=Genotype A, **G**=Genotype  
625 D, **H**=Genotype E) and infected patient tissue (**I**=P1) (Blue = Unmethylated CpG site,  
626 Red = Methylated CpG site), (CpGI=CpG Islands detected with Meth primer).

627

628 **Figure 3.** Epigenetic heterogeneity in HBV from infected patients. **A:** Variability of  
629 5mC levels in a random selection of single HBV molecules. **B:** K-means clustering of  
630 HBV molecules. **C:** heatmap clustering of single HBV molecules.

631

## 632 **References**

- Ancey, Pierre-Benoit, Barbara Testoni, Marion Gruffaz, Marie-Pierre Cros, Geoffroy Durand, Florence Le Calvez-Kelm, David Durantel, Zdenko Herceg, and Hector Hernandez-Vargas. 2015. "Genomic Responses to Hepatitis B Virus (HBV) Infection in Primary Human Hepatocytes." *Oncotarget* 6(42):44877–91.
- Chen, Chien-Jen. 2006. "Risk of Hepatocellular Carcinoma Across a Biological Gradient of Serum Hepatitis B Virus DNA Level." *JAMA* 295(1):65.
- Cohen, Damien, Sumantra Ghosh, Yusuke Shimakawa, Njie Ramou, Pierre Simon Garcia, Anaëlle Dubois, Clément Guillot, Nora Kakwata-Nkor Deluce, Valentin Tilloy, Geoffroy Durand, Catherine Voegele, Gibril Ndow, Umberto d'Alessandro, Céline Brochier-Armanet, Sophie Alain, Florence Le Calvez-Kelm, Janet Hall, Fabien Zoulim, Maimuna Mendy, Mark Thursz, Maud Lemoine, and Isabelle Chemin. 2020. "HBV PreS2Δ38-55 Variants: A Newly Identified Risk Factor for Hepatocellular Carcinoma." *JHEP Reports* 100144.
- De Coster, Wouter, Endre Bakken Stovner, and Mojca Strazisar. 2020. "Methplotlib: Analysis of Modified Nucleotides from Nanopore Sequencing" edited by A. Valencia. *Bioinformatics* 36(10):3236–38.
- Fernandez, Agustin F., Cecilia Rosales, Pilar Lopez-Nieva, Osvaldo Graña, Esteban Ballestar, Santiago Ropero, Jesus Espada, Sonia A. Melo, Amaia Lujambio, Mario F. Fraga, Irene Pino, Biola Javierre, Francisco J. Carmona, Francesco Acquadro, Renske D. M. Steenbergen, Peter J. F. Snijders, Chris J. Meijer, Pascal Pineau, Anne Dejean, Belen Lloveras, Gabriel Capella, Josep Quer, Maria Buti, Juan-Ignacio Esteban, Helena Allende, Francisco Rodriguez-Frias, Xavier Castellsague, Janos Minarovits, Jordi Ponce, Daniela Capello, Gianluca Gaidano, Juan Cruz Cigudosa, Gonzalo Gomez-Lopez, David G. Pisano, Alfonso Valencia, Miguel Angel Piris, Francesc X. Bosch, Ellen Cahir-McFarland, Elliott Kieff, and Manel Esteller. 2009. "The Dynamic DNA Methylomes of Double-Stranded DNA Viruses Associated with Human Cancer." *Genome Research* 19(3):438–51.
- Ghosh, Sourav, Shantanu Sengupta, and Vinod Scaria. 2014. "Comparative Analysis of Human Mitochondrial Methylomes Shows Distinct Patterns of Epigenetic Regulation in Mitochondria." *Mitochondrion* 18:58–62.
- Gigante, Scott, Quentin Gouil, Alexis Lucattini, Andrew Keniry, Tamara Beck, Matthew Tinning, Lavinia Gordon, Chris Woodruff, Terence P. Speed, Marnie E. Blewitt, and Matthew E. Ritchie. 2019. "Using Long-Read Sequencing to Detect Imprinted DNA Methylation." *Nucleic Acids Research* 47(8):e46–e46.
- Gilpatrick, Timothy, Isac Lee, James E. Graham, Etienne Raimondeau, Rebecca Bowen, Andrew Heron, Bradley Downs, Saraswati Sukumar, Fritz J. Sedlazeck, and Winston Timp. 2020. "Targeted Nanopore Sequencing with Cas9-Guided Adapter Ligation." *Nature Biotechnology* 38(4):433–38.

- Guo, Yanhai, Yongnian Li, Shijie Mu, Ju Zhang, and Zhen Yan. 2009. "Evidence That Methylation of Hepatitis B Virus Covalently Closed Circular DNA in Liver Tissues of Patients with Chronic Hepatitis B Modulates HBV Replication." *Journal of Medical Virology* 81(7):1177–83.
- Hernandez, Hector, and Chloe Goldsmith. n.d. "Quantitative Analysis of Methylation and Hydroxymethylation Using OXBS-QMSP v1 (Protocols.Io.52bg8an)."
- Ikedo, K., M. Kobayashi, T. Someya, S. Saitoh, T. Hosaka, N. Akuta, F. Suzuki, Y. Suzuki, Y. Arase, and H. Kumada. 2009. "Occult Hepatitis B Virus Infection Increases Hepatocellular Carcinogenesis by Eight Times in Patients with Non-B, Non-C Liver Cirrhosis: A Cohort Study." *Journal of Viral Hepatitis* 16(6):437–43.
- Jain, Miten, Hugh E. Olsen, Benedict Paten, and Mark Akeson. 2016. "The Oxford Nanopore MinION: Delivery of Nanopore Sequencing to the Genomics Community." *Genome Biology* 17(1):239.
- Koren, Sergey, Brian P. Walenz, Konstantin Berlin, Jason R. Miller, Nicholas H. Bergman, and Adam M. Phillippy. 2017. "Canu: Scalable and Accurate Long-Read Assembly via Adaptive k-Mer Weighting and Repeat Separation." *Genome Research* 27(5):722–36.
- Lebossé, Fanny, Barbara Testoni, Judith Fresquet, Floriana Facchetti, Enrico Galmozzi, Maëlen Fournier, Valérie Hervieu, Pascale Berthillon, Françoise Berby, Isabelle Bordes, David Durantel, Massimo Levrero, Pietro Lampertico, and Fabien Zoulim. 2017. "Intrahepatic Innate Immune Response Pathways Are Downregulated in Untreated Chronic Hepatitis B." *Journal of Hepatology* 66(5):897–909.
- Leger, Adrien, and Tommaso Leonardi. 2019. "PycoQC, Interactive Quality Control for Oxford Nanopore Sequencing." *Journal of Open Source Software* 4(34):1236.
- Lemoine, Maud, Yusuke Shimakawa, Ramou Njie, Makie Taal, Gibril Ndow, Isabelle Chemin, Sumantra Ghosh, Harr F. Njai, Adam Jeng, Amina Sow, Coumba Toure-Kane, Souleymane Mboup, Penda Suso, Saydiba Tamba, Abdullah Jatta, Louise Sarr, Aboubacar Kambi, William Stanger, Shevanthi Nayagam, Jessica Howell, Liliane Mpabanzi, Ousman Nyan, Tumani Corrah, Hilton Whittle, Simon D. Taylor-Robinson, Umberto D'Alessandro, Maimuna Mendy, and Mark R. Thursz. 2016. "Acceptability and Feasibility of a Screen-and-Treat Programme for Hepatitis B Virus Infection in The Gambia: The Prevention of Liver Fibrosis and Cancer in Africa (PROLIFICA) Study." *The Lancet Global Health* 4(8):e559–67.
- Li, Yuanyuan, and Trygve O. Tollefsbol. 2011. "DNA Methylation Detection: Bisulfite Genomic Sequencing Analysis." *Methods in Molecular Biology (Clifton, N.J.)* 791:11–21.
- Liu, Yibin, Jingfei Cheng, Paulina Siejka-Zielińska, Carika Weldon, Hannah Roberts, Maria Lopopolo, Andrea Magri, Valentina D'Arienzo, James M. Harris, Jane A. McKeating, and Chun-Xiao Song. 2020. "Accurate Targeted Long-Read DNA Methylation and Hydroxymethylation Sequencing with TAPS." *Genome Biology* 21(1):54.
- Lu, Hengyun, Francesca Giordano, and Zemin Ning. 2016. "Oxford Nanopore MinION Sequencing and Genome Assembly." *Genomics, Proteomics & Bioinformatics* 14(5):265–79.

- Madoui, Mohammed-Amin, Stefan Engelen, Corinne Cruaud, Caroline Belser, Laurie Bertrand, Adriana Alberti, Arnaud Lemainque, Patrick Wincker, and Jean-Marc Aury. 2015. "Genome Assembly Using Nanopore-Guided Long and Error-Free DNA Reads." *BMC Genomics* 16:327.
- Mak, Lung-Yi, Danny Ka-Ho Wong, Teresa Pollicino, Giovanni Raimondo, F. Blaine Hollinger, and Man-Fung Yuen. 2020. "Occult Hepatitis B Infection and Hepatocellular Carcinoma: Epidemiology, Virology, Hepatocarcinogenesis and Clinical Significance." *Journal of Hepatology*.
- Martel, Nora, Selma A. Gomes, Isabelle Chemin, Christian Trépo, and Alan Kay. 2013. "Improved Rolling Circle Amplification (RCA) of Hepatitis B Virus (HBV) Relaxed-Circular Serum DNA (RC-DNA)." *Journal of Virological Methods* 193(2):653–59.
- Mirabello, Lisa, Chang Sun, Arpita Ghosh, Ana C. Rodriguez, Mark Schiffman, Nicolas Wentzensen, Allan Hildesheim, Rolando Herrero, Sholom Wacholder, Attila Lorincz, and Robert D. Burk. 2012. "Methylation of Human Papillomavirus Type 16 Genome and Risk of Cervical Precancer in a Costa Rican Population." *Journal of the National Cancer Institute* 104(7):556–65.
- Nakamura, Takuya, Jun Inoue, Masashi Ninomiya, Eiji Kakazu, Tomoaki Iwata, Satoshi Takai, Akitoshi Sano, Takayuki Kogure, Tooru Shimosegawa, and Atsushi Masamune. 2020. "Effect of Viral DNA Methylation on Expression of Hepatitis B Virus Proteins Depends on the Virus Genotype." *Virus Genes* 56(4):439–47.
- Njai, Harr Freeya, Yusuke Shimakawa, Bakary Sanneh, Lynne Ferguson, Gibril Ndow, Maimuna Mendy, Amina Sow, Gora Lo, Coumba Toure-Kane, Junko Tanaka, Makie Taal, Umberto D'alessandro, Ramou Njie, Mark Thursz, and Maud Lemoine. 2015. "Validation of Rapid Point-of-Care (POC) Tests for Detection of Hepatitis B Surface Antigen in Field and Laboratory Settings in the Gambia, Western Africa." *Journal of Clinical Microbiology* 53(4):1156–63.
- Nurk, Sergey, Brian P. Walenz, Arang Rhie, Mitchell R. Vollger, Glennis A. Logsdon, Robert Grothe, Karen H. Miga, Evan E. Eichler, Adam M. Phillippy, and Sergey Koren. 2020. "HiCanu: Accurate Assembly of Segmental Duplications, Satellites, and Allelic Variants from High-Fidelity Long Reads." *Genome Research* gr.263566.120.
- Olkhov-Mitsel, Ekaterina, and Bharati Bapat. 2012. "Strategies for Discovery and Validation of Methylated and Hydroxymethylated DNA Biomarkers." *Cancer Medicine* 1(2):237–60.
- Park, Yongseok, and Hao Wu. 2016. "Differential Methylation Analysis for BS-Seq Data under General Experimental Design." *Bioinformatics* 32(10):1446–53.
- Payne, Alexander, Nadine Holmes, Thomas Clarke, Rory Munro, Bisrat Debebe, and Matthew Loose. 2020. *Nanopore Adaptive Sequencing for Mixed Samples, Whole Exome Capture and Targeted Panels*. preprint. Genomics.
- Pollicino, Teresa, Laura Belloni, Giuseppina Raffa, Natalia Pediconi, Giovanni Squadrito, Giovanni Raimondo, and Massimo Levrero. 2006. "Hepatitis B Virus Replication Is Regulated by the Acetylation Status of Hepatitis B Virus CccDNA-Bound H3 and H4 Histones." *Gastroenterology* 130(3):823–37.

- Quick, Joshua, Nicholas J. Loman, Sophie Duraffour, Jared T. Simpson, Ettore Severi, Lauren Cowley, Joseph Akoi Bore, Raymond Koundouno, Gytis Dudas, Amy Mikhail, Nobila Ouédraogo, Babak Afrough, Amadou Bah, Jonathan H. J. Baum, Beate Becker-Ziaja, Jan Peter Boettcher, Mar Cabeza-Cabrerizo, Álvaro Camino-Sánchez, Lisa L. Carter, Juliane Doerrbecker, Theresa Enkirch, Isabel García-Dorival, Nicole Hetzelt, Julia Hinzmann, Tobias Holm, Liana Eleni Kafetzopoulou, Michel Koropogui, Abigael Kosgey, Eeva Kuisma, Christopher H. Logue, Antonio Mazzarelli, Sarah Meisel, Marc Mertens, Janine Michel, Didier Ngabo, Katja Nitzsche, Elisa Pallasch, Livia Victoria Patrono, Jasmine Portmann, Johanna Gabriella Repits, Natasha Y. Rickett, Andreas Sachse, Katrin Singethan, Inês Vitoriano, Rahel L. Yemanaberhan, Elsa G. Zekeng, Trina Racine, Alexander Bello, Amadou Alpha Sall, Ousmane Faye, Oumar Faye, N’Faly Magassouba, Cecelia V. Williams, Victoria Amburgey, Linda Winona, Emily Davis, Jon Gerlach, Frank Washington, Vanessa Monteil, Marine Jourdain, Marion Bererd, Alimou Camara, Hermann Somlare, Abdoulaye Camara, Marianne Gerard, Guillaume Bado, Bernard Baillet, Déborah Delaune, Koumpingnin Yacouba Nebie, Abdoulaye Diarra, Yacouba Savane, Raymond Bernard Pallawo, Giovanna Jaramillo Gutierrez, Natacha Milhano, Isabelle Roger, Christopher J. Williams, Facinet Yattara, Kuiama Lewandowski, James Taylor, Phillip Rachwal, Daniel J. Turner, Georgios Pollakis, Julian A. Hiscox, David A. Matthews, Matthew K. O’ Shea, Andrew McD. Johnston, Duncan Wilson, Emma Hutley, Erasmus Smit, Antonino Di Caro, Roman Wölfel, Kilian Stoecker, Erna Fleischmann, Martin Gabriel, Simon A. Weller, Lamine Koivogui, Boubacar Diallo, Sakoba Keïta, Andrew Rambaut, Pierre Formenty, Stephan Günther, and Miles W. Carroll. 2016. “Real-Time, Portable Genome Sequencing for Ebola Surveillance.” *Nature* 530(7589):228–32.
- Raimondo, G., T. Pollicino, L. Romanò, and A. R. Zanetti. 2010. “A 2010 Update on Occult Hepatitis B Infection.” *Pathologie Biologie* 58(4):254–57.
- Raimondo, Giovanni, Stephen Locarnini, Teresa Pollicino, Massimo Levrero, Fabien Zoulim, Anna S. Lok, and Taormina Workshop on Occult HBV Infection Faculty Members. 2019. “Update of the Statements on Biology and Clinical Impact of Occult Hepatitis B Virus Infection.” *Journal of Hepatology* 71(2):397–408.
- Rajoriya, Neil, Christophe Combet, Fabien Zoulim, and Harry L. A. Janssen. 2017. “How Viral Genetic Variants and Genotypes Influence Disease and Treatment Outcome of Chronic Hepatitis B. Time for an Individualised Approach?” *Journal of Hepatology* 67(6):1281–97.
- Rodríguez-Aguilera, Jesús Rafael, Szilvia Ecsedi, Marie-Pierre Cros, Chloe Goldsmith, Mariana Domínguez-López, Nuria Guerrero-Celis, Rebeca Pérez-Cabeza de Vaca, Isabelle Chemin, Félix Recillas-Targa, Victoria Chagoya de Sánchez, and Héctor Hernández-Vargas. 2019. *Genome-Wide 5-Hydroxymethylcytosine (5hmC) Emerges at Early Stage of in Vitro Hepatocyte Differentiation. preprint.* Genomics.
- Simpson, Jared T., Rachael E. Workman, P. C. Zuzarte, Matei David, L. J. Dursi, and Winston Timp. 2017. “Detecting DNA Cytosine Methylation Using Nanopore Sequencing.” *Nature Methods* 14(4):407–10.
- Testoni, Barbara, Fanny Lebossé, Caroline Scholtes, Françoise Berby, Clothilde Miaglia, Miroslava Subic, Alessandro Loglio, Floriana Facchetti, Pietro Lampertico, Massimo Levrero, and Fabien

- Zoulim. 2019. “Serum Hepatitis B Core-Related Antigen (HBcrAg) Correlates with Covalently Closed Circular DNA Transcriptional Activity in Chronic Hepatitis B Patients.” *Journal of Hepatology* 70(4):615–25.
- Viehweger, Adrian, Sebastian Krautwurst, Kevin Lamkiewicz, Ramakanth Madhugiri, John Ziebuhr, Martin Hölzer, and Manja Marz. 2019. “Direct RNA Nanopore Sequencing of Full-Length Coronavirus Genomes Provides Novel Insights into Structural Variants and Enables Modification Analysis.” *Genome Research* 29(9):1545–54.
- Vivekanandan, P., D. Thomas, and M. Torbenson. 2008. “Hepatitis B Viral DNA Is Methylated in Liver Tissues.” *Journal of Viral Hepatitis* 15(2):103–7.
- Vivekanandan, Perumal, Rajesh Kannangai, Stuart C. Ray, David L. Thomas, and Michael Torbenson. 2008. “Comprehensive Genetic and Epigenetic Analysis of Occult Hepatitis B from Liver Tissue Samples.” *Clinical Infectious Diseases* 46(8):1227–36.
- Wang, G. H., and C. Seeger. 1993. “Novel Mechanism for Reverse Transcription in Hepatitis B Viruses.” *Journal of Virology* 67(11):6507–12.
- Xia, Yuchen, and Haitao Guo. 2020. “Hepatitis B Virus CccDNA: Formation, Regulation and Therapeutic Potential.” *Antiviral Research* 180:104824.
- Xia, Yuchen, Daniela Stadler, Chunkyu Ko, and Ulrike Protzer. 2017. “Analyses of HBV CccDNA Quantification and Modification.” Pp. 59–72 in *Hepatitis B Virus*. Vol. 1540, *Methods in Molecular Biology*, edited by H. Guo and A. Cuconati. New York, NY: Springer New York.
- Zhang, Zheng, Scott Schwartz, Lukas Wagner, and Webb Miller. 2000. “A Greedy Algorithm for Aligning DNA Sequences.” *Journal of Computational Biology* 7(1–2):203–14.

## Supplementary Figure Legends

633 **Supplementary figure 1.** A and B: Yield for aligned reads calculated with pycoQC  
634 (representative sample). C: Coverage of HBV identifying the Gap in HBV reads. D:  
635 HBV genotype was determined by jumping profile Hidden Markov Model (jpHMM). E-F:  
636 Infection efficacy for HBV genotypes. PHH were infected with 100MOI of HBV genotype  
637 A, E or D. Serum levels of HBsAg, HBeAg were quantified by ELISA and HBV DNA was  
638 quantified by qPCR after 0, 3 and 6 days post infection.

639 **Supplementary figure 2.** PHRED scores for nanopore runs. A: Genotype A  
640 sequenced on MinION, B: Genotype D sequenced on MinION, C: Genotype E  
641 sequenced on MinION, D: Genotype D sequenced on Flongle.

## Supplementary Table Legends

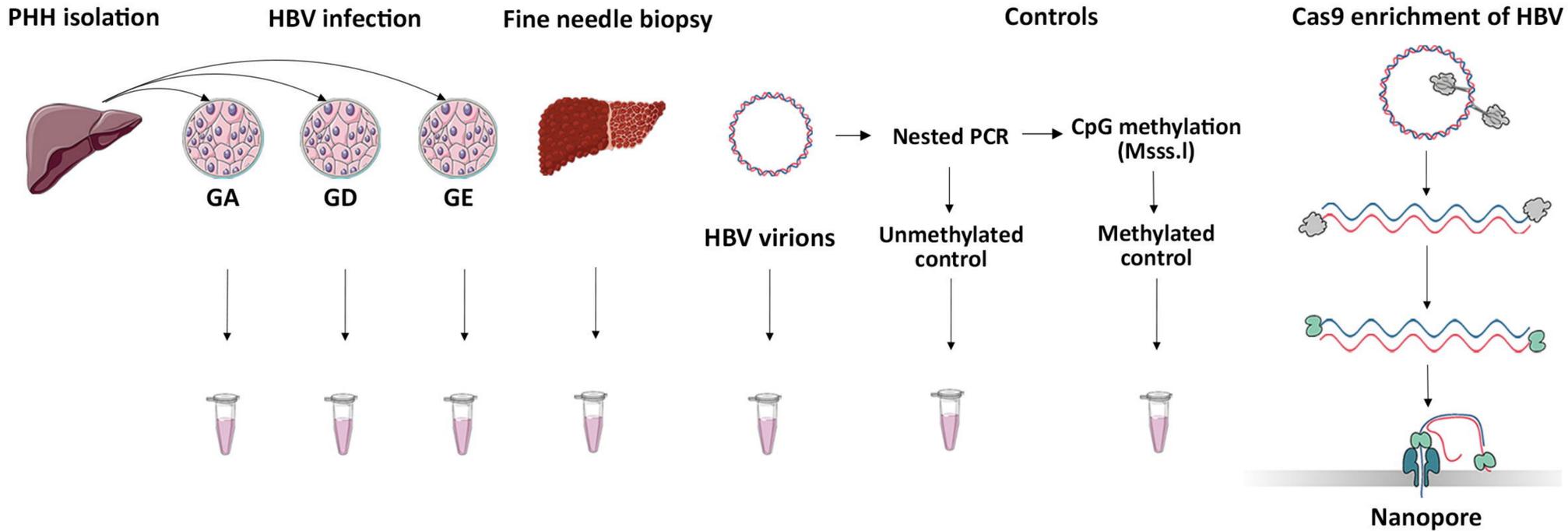
642 **Supplementary table 1.** Sequencing depth for effective calculation of HBV 5mCpG  
643 levels: p-value table corresponding to figure 1B.

644 **Supplementary table 2.** Primer sequences for BS-qMSP of HBV.

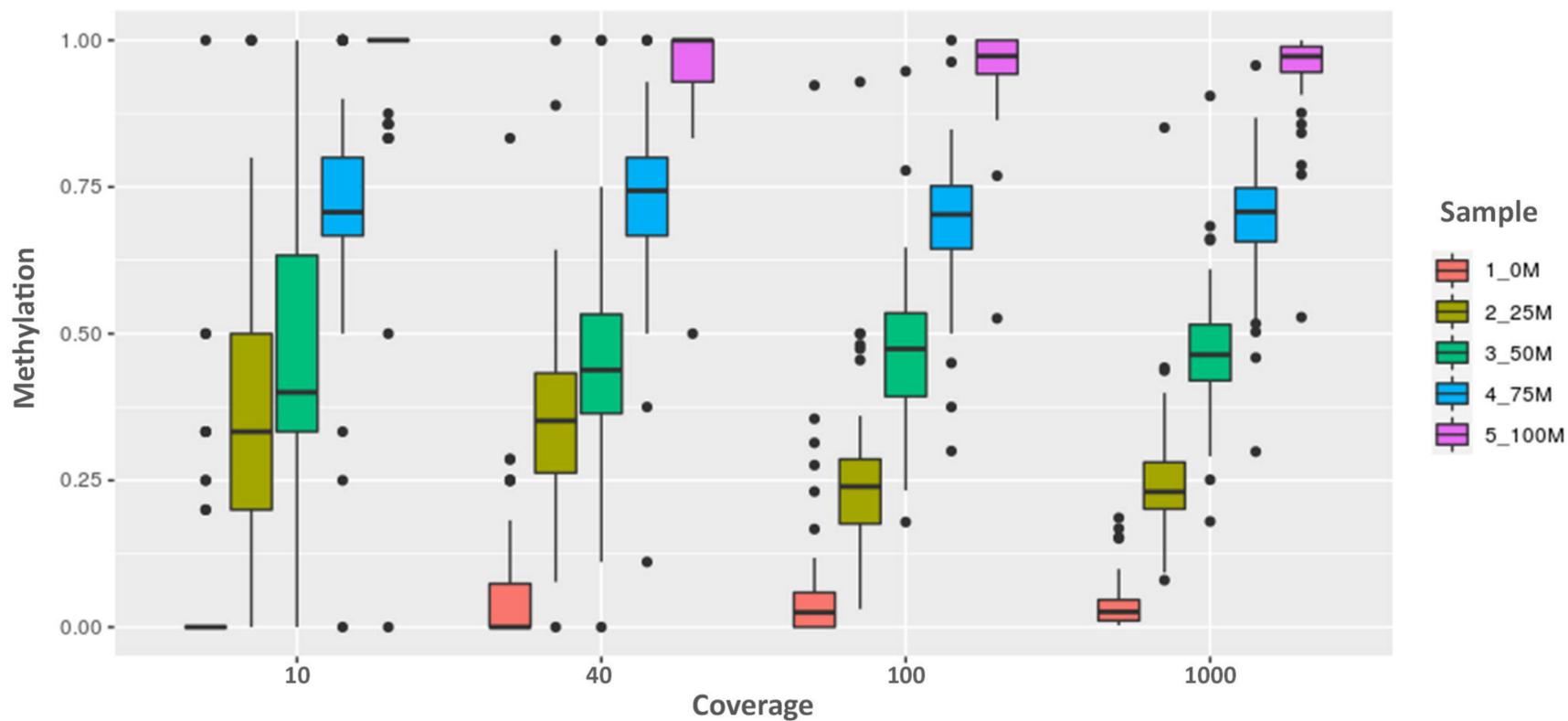
645

Figure 1

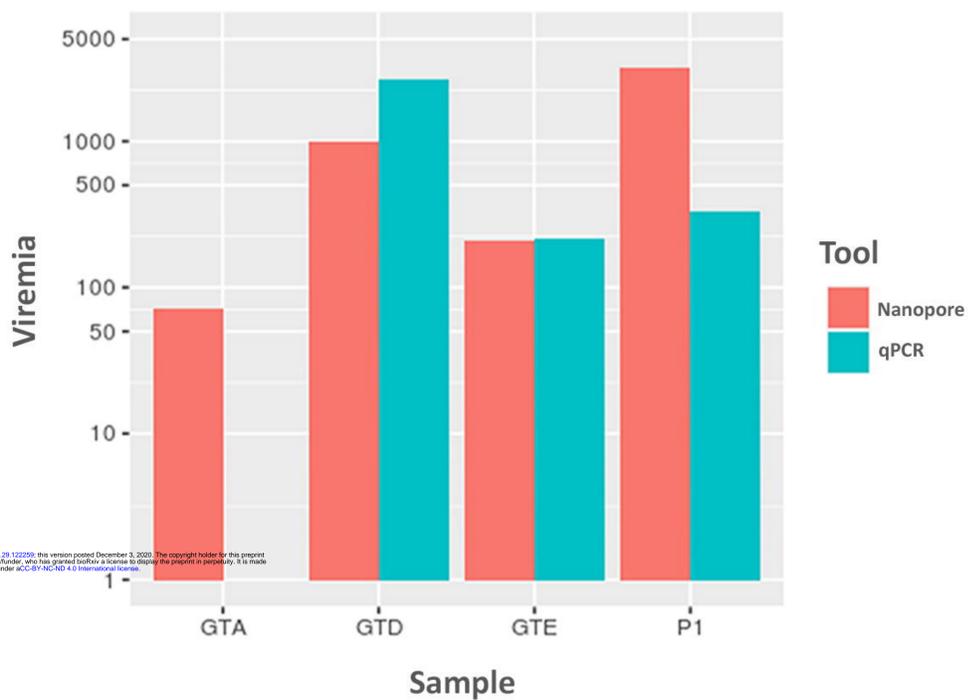
**A**



**B**



**C**



**D**

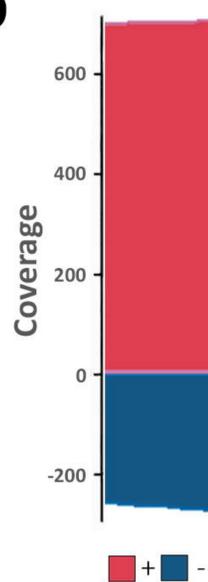


**Figure 2**

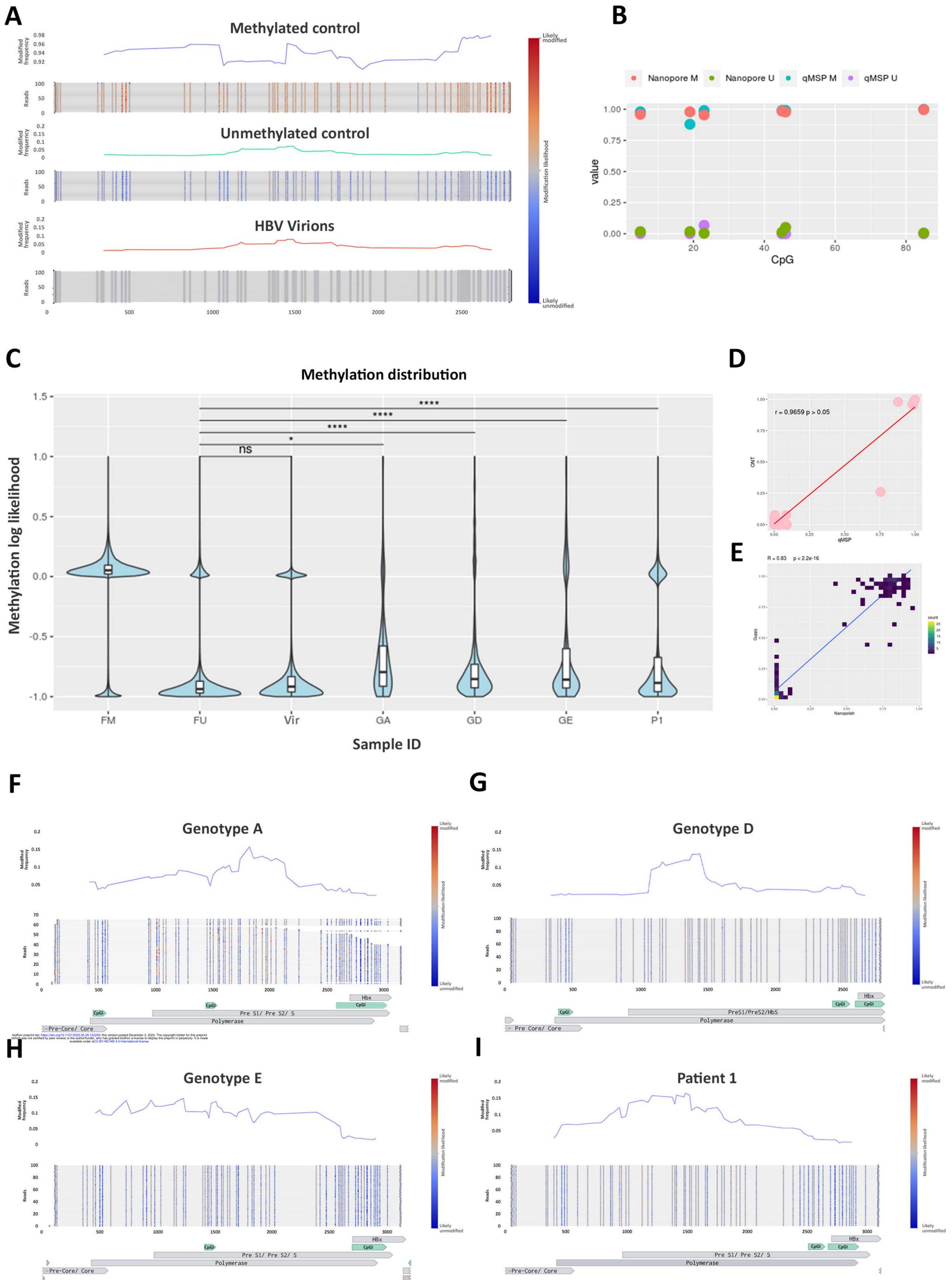


Figure 3

